Neuroanatomical evaluation of periprostatic nerve in patients submitted to nerve-sparing prostatectomy at 3T: feasibility study and preliminary experience

V. Panebianco[1], S. Prato [2], D. Lisi[1], V. Buonocore[1], T. Biondi[1], and R. Passariello[1]
[1]Department of Radiological Sciences, Sapienza University, Rome, Italy, [2]MR Advanced Applications, GE Healthcare, Milan, Italy

INTRODUCTION: the neuroanatomical evaluation of the periprostatic nerve has high clinical impact in patients submitted to nerve-sparing prostatectomy (NSP). Radical Retro-pubic Prostatectomy (RRP) provides excellent long-term cancer control for patients with clinically localized prostate carcinoma [1]. Erectile dysfunction (ED) is one of the complications after RRP and the recovery of erectile function is quantitatively related to the preservation of the neurovascular bundles (NVBs) [2]. Magnetic resonance imaging (MRI) provides excellent depiction of the pelvic anatomy and has also been shown to be useful in predicting the extension of prostate cancer to the NVBs in pre-surgical evaluation [3, 4, and 5]. In the post-surgery evaluation 3D T2 imaging is able to depict changes of NVBs [6]. The aim of this study is to depict the neuroanatomical distribution and relationship with capsular profile of periprostatic nerve in patients submitted to a bilateral NSP using Diffusion Tensor Imaging (DTI) and tracing the spatial orientation of the fibers.

SUBJECTS and METHODS: thirty-tree patients candidates for prostatectomy have been studied, 36% of the patients were candidate for nerve sparing prostatectomy, 25% of them with bilateral nerve sparing prostatectomy. Patients underwent MR examination at 3T magnet (Discovery MR750, GE Healthcare, Waukesha, WI) using 8ch Body Phase Array Coil combined with endo-rectal coil (e-Coil, Medrad). Single Shot Spin Echo EPI has been selected for DTI imaging due to its high acquisition speed and the diffusion weighted gradients were applied in 16 directions with a b-value of 1000s/mm^2. In order to reduce signal loss due to relaxations effects, we used the minimum echo time (TE), using of the maximal slew rate (200 T/m/s), without exceeding the regulatory limit for peripheral nerve stimulation. The use of a SENSE based parallel imaging with acceleration factor of 2 reduced susceptibility–induced artifacts by reducing the echo train length and thereby the amounts of time that the off-resonant spins accumulate phase errors. A localized shimming volume was localized accurately on the prostate in order to exclude the air inflated in the endo-rectal coil, the size of the shim volume was varying based on the prostate size. The use of the shortest TE, of the parallel imaging and a localized shim volume were necessary to reduce geometric distortions due to phase accumulation in the EPI acquisitions and magnetic susceptibility variations due to the air in the coil. DTI data were post processed using Fctl FiberTracking (GE Healthcare). Fibertracking images were fused with anatomical T2 FRFSE images.

RESULTS and DISCUSSION: In all patients the tractography of the periprostatic nerve was able to demonstrate the integrity of the nerve fibers and relationship of the lesion with the nerve before RRP. In Figure1 the periprostatic nerve is adjacent to the lesion while in Figure 3 the fibertraking imaging shows distance between the nerve and the lesion, supporting the surgeon during the decision making process. Figure 2 illustrates in a patient the course and the distribution of the left periprostatic nerve along the posterior capsular profile of the prostate. In Figure 4 Antero-superior oblique view of the tractography demonstrating the asymmetry of the course and the distribution of the right and left nerve fibers after HIFU therapy.

CONCLUSION: Fibertracking with endorectal coil of the periprostatic nerve is a feasible application, obtaining a precise neuroanatomical evaluation of the periprostatic nerve in terms of: distance from nerve fiber to prostate capsular profile, distance from nerve fiber to the lesion and integrity and course of the nerve on each part of the prostate.

REFERENCES: 1. Hull GW et All. J Urol 167(2 Pt 1):528–534; 2. Rabbani F, et All J Urol 164:1929–1934; 3. Bloch BN et All Radiology 245(1):176–85; 4. Ogura K, Urology 57:721–726; 5. Hricak H et All, Cancer 100:2655–2663; 6. Panebianco V. et All Eur Radiol. 2009 Jan;19(1):220-9.

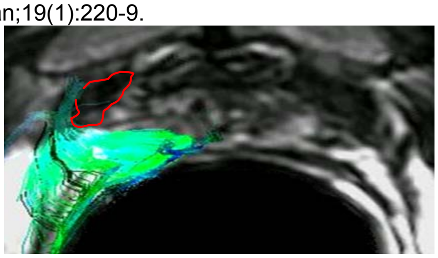

Fig.1: Case 1 Periprostatic nerve adjacent to prostate lesion outline in red.

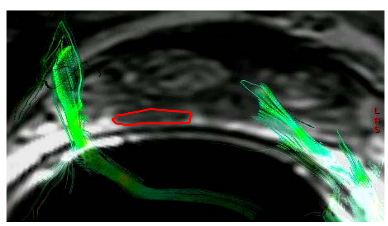

Fig.3: Case 3 Tractography showing distance between the nerve and the lesion outlined in red.

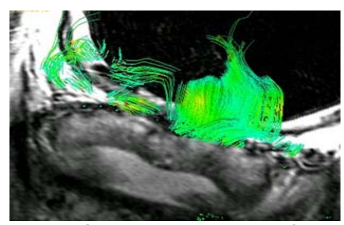

Fig.4: Case 4 Asymmetry of the course and the distribution of the right nerves

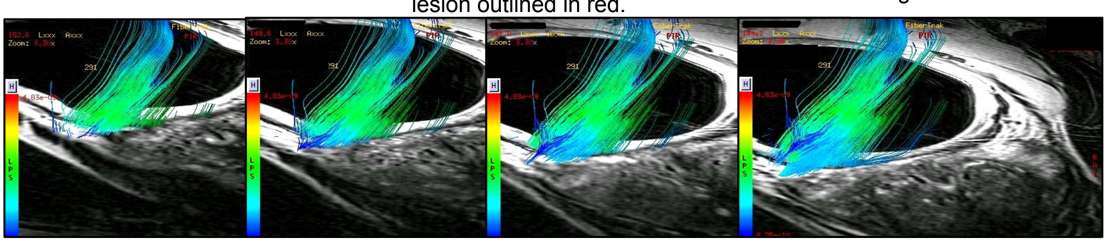

Fig.2 - Case 2 Antero-superior view of the tractography illustrating the course and distribution of the left nerve